# Investigation of the Performance Degradation of 4H-SiC Neutron Detectors Using MCNP and TCAD

Yongbo Sun, Zhimeng Hu, Hui Zhang, Pin Gong, Guoqiang Zhong, Liqun Hu, Giuseppe Gorini, Gabriele Croci, and Xiaobin Tang

***Abstract*—4H-SiC belongs to the family of the third-generation semiconductors and features excellent properties, e.g., high radiation resistance, high charge collection efficiency (CCE), exceptional thermal stability, and low sensitivity to $\gamma$-rays. These advantages make 4H-SiC suitable for developing neutron detectors used in intense neutron fields characteristic of tokamaks. However, 4H-SiC detectors suffer from performance degradation after neutron irradiation to high fluence. The knowledge of the degradation evolution of 4H-SiC detector performance parameters with neutron fluence in specific situations can not only help optimize the detector design but also help understand and even correct experimental data for its better use. The technology computer-aided design (TCAD) software is used here to predict the detailed parameters in 4H-SiC bulk underlying the detector performance degradation resulting from neutron irradiations in the vicinity of experimental advanced superconducting tokamak (EAST) tokamak, a fusion device, and the reason for the detector performance degradation caused by neutron irradiation is analyzed. Our 4H-SiC detector damage analysis model employed in TCAD yields CCE values, which have a reasonable consistency with experimental results obtained in references for neutron fluences up to 5 × $10^{15}$ $cm^{-2}$. Additionally, at the neutron fluence of $10^{15}$ $cm^{-2}$, the electric fields within 4H-SiC bulk have significant distortions. Nonetheless, the CCE remains at about 40%, demonstrating an extremely high tolerance to neutron irradiations. Meanwhile, our study reveals that enhancing carrier transport rates and strengthening the field within the sensitive region can effectively mitigate the degradation of detector performance, thereby enhancing the detector's radiation tolerance.**

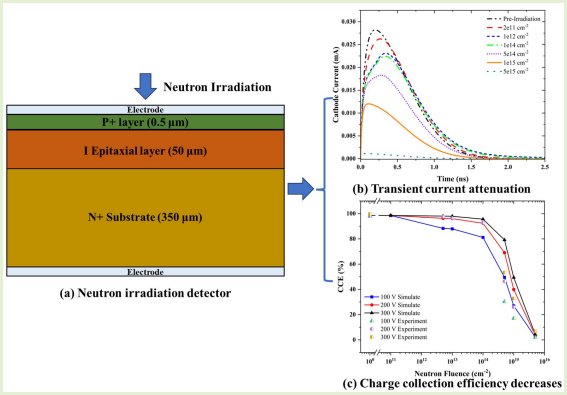


***Index Terms*—4H-SiC detector, charge collection efficiency (CCE), fusion neutron, radiation damage, technology computer-aided design (TCAD).**

Manuscript received 24 November 2023; revised 16 December 2023; accepted 17 December 2023. Date of publication 1 January 2024; date of current version 13 February 2024. This work was supported in part by the National Natural Science Foundation of China under Grant 12105144 and Grant 12375297, in part by the Primary Research and Development Plan of Jiangsu Province under Grant BE2022846 and Grant BE2023816, in part by the China Postdoctoral Science Foundation under Grant 2022M721659, and in part by the Fundamental Research Funds for the Central Universities under Grant NG2023002 and Grant NC2022006. The associate editor coordinating the review of this article and approving it for publication was Dr. Richard T. Kouzes. *(Corresponding authors: Zhimeng Hu; Xiaobin Tang.)*

Yongbo Sun, Zhimeng Hu, Pin Gong, and Xiaobin Tang are with the Department of Nuclear Science and Technology, Nanjing University of Aeronautics and Astronautics, Nanjing 210016, China, and also with the Key Laboratory of Nuclear Technology Application and Radiation Protection in Astronautics, Ministry of Industry and Information Technology, Nanjing University of Aeronautics and Astronautics, Nanjing 211106, China (e-mail: huzhm21@nuaa.edu.cn; tangxiaobin@nuaa.edu.cn).

Hui Zhang is with the National Institute of Metrology, Beijing 100029, China.

Guoqiang Zhong and Liqun Hu are with the Institute of Plasma Physics, Chinese Academy of Sciences, Hefei 230031, China.

Giuseppe Gorini and Gabriele Croci are with the Department of Physics, University of Milan-Bicocca, 20126 Milan, Italy.

Digital Object Identifier 10.1109/JSEN.2023.3345407

## I. Introduction

In MAGNETIC confinement fusion plasmas, neutrons are generated through nuclear reactions $D(d,n)^3$He and $T(d,n)^4$He. By measuring the number and energy spectrum of neutrons produced in fusion reactions, different plasma parameters related to the velocity distribution of fast ions can be obtained [1], [2], [3]. Accurately obtaining plasma parameters is of paramount importance for research in plasma physics and the stable operation of fusion devices [4]. In a single discharge experiment of tokamak devices, the neutron yield can exceed $10^{19}$ $s^{-1}$ [5], [6]. Neutron flux can surpass $10^{11}$ $cm^{-2} \cdot s^{-1}$ at positions several meters away from the plasma center. The present silicon and scintillation detectors are only resistant to neutron irradiations at the level of $10^{12}$ $cm^{-2}$ and have difficulty meeting the requirements of stable operation for long-term use [7], [8]. In addition to high neutron fluences, the harsh working conditions around fusion devices consist of strong magnetic fields and high $\gamma$-ray backgrounds. Therefore, the development of neutron-tolerant

detectors that can withstand the harsh operating conditions in fusion experiments has become a crucial issue [4].

4H-SiC material features a wide bandgap (3.27 eV), a high displacement threshold energy (21.8 eV), and excellent electrical and thermal properties. Therefore, 4H-SiC detectors can operate in environments with high temperatures and intense neutron radiation, making them potential detectors for fusion neutron measurements [9], [10], [11]. 4H-SiC is used in p-i-n junction diode or Schottky barrier diode (SBD) detectors [10]. They can be utilized for direct neutron energy spectrum measurements through nonelastic and elastic scattering reactions with $^{12}$C nuclei in the detector bulk [7]. Alternatively, they can be coated with thermal neutron conversion materials, such as $^{6}$LiF and $B_4C$ on their electrode surfaces, to be used as thermal neutron counters. Placing these counters within moderator materials like polyethylene can also develop neutron monitors or broad-energy neutron spectrometers [10]. Research indicates that 4H-SiC detectors exhibit energy resolution, detection efficiency, and extremely high charge collection efficiency (CCE) comparable to diamond detectors [12], [13]. Compared to silicon, the larger bandgap width of 4H-SiC results in significantly lower leakage and noise, enabling its stable operation under high temperature up to 700 °C [9]. The high displacement threshold energy of 4H-SiC also suppresses the generation of internal defects during irradiation, imparting exceptional radiation stability to 4H-SiC detectors.

Numerous studies have shown that 4H-SiC detectors maintain good performance even after exposure to neutrons exceeding $10^{14}$ cm$^{-2}$ [14], [15]. However, experiments also revealed that the performance degradation of 4H-SiC detectors still occurred when the neutron fluence was less than $10^{14}$ cm$^{-2}$ and the degradation becomes worse with increasing fluence [14]. The irradiation damage distorts the electric field in the sensitive region of 4H-SiC detectors, which influences the charge carrier transport, leading to the current pulse signal distortion, CCE decrease, energy resolution deterioration, and even counting rate decrease [12], [14], [15], [16], [17]. Many experiments have been carried out to investigate the performance degradation of semiconductor detectors under neutron irradiations [12], [14]. The superiority of simulation methods to experiments is the low cost as large facilities for producing intense neutrons are not needed [18], [19] and the flexibility in adjusting source parameters and in constructing detectors with different geometries and manufacturing processes [20], [21]. The simulation methods can thus give more detailed performance parameters that it is hard or impossible to give via experiments, e.g., electric field distribution in the detector's sensitive region, carrier drift and recombination at different positions, and CCE in specific time or neutron fluence [17], [22]. The parameters predicted using simulations can be utilized to correct data from detectors and guide the design optimization of detectors [23], [24], thus enhancing the accuracy of detector counts and pulse height spectra used for understanding and controlling fusion burning plasmas in fusion devices.

The technology computer-aided design (TCAD) simulation method has already been used in the research of 4H-SiC detector performance. For instance, Tripathi et al. [18] utilized TCAD to study the impact of gamma and neutron irradiation on the electrical performance of 4H-SiC fast neutron detectors. Siddiqui and Usman [23] conducted a comparative study using TCAD to investigate the proton radiation tolerance of both silicon and SiC detectors. Xiong et al. [24] employed TCAD to analyze the charge collection characteristics of SiC fast neutron detectors. Zhang et al. [25] used TCAD to investigate the detector output characteristics when detecting heavy charged particles with SiC detectors. The aforementioned work primarily uses simulation programs to conduct carrier transport simulations and performance analysis in semiconductor detectors, as well as to analyze the electrical characteristics, such as $I$–$V$ and $C$–$V$ of 4H-SiC detectors after exposure to neutrons, protons, and gamma irradiation. However, there is still a lack of research on the performance degradation evolution for 4H-SiC detectors after exposure to high neutron fluences.

This study simulated the electric field distortion in the sensitive region and the performance degradation evolution of 4H-SiC detectors under neutron irradiation in the experimental advanced superconducting tokamak (EAST) tokamak. First, Monte Carlo N–Particle Transport Code System 6 (MCNP6) was used to optimize the design of 4H-SiC neutron detectors suitable for neutron monitoring in a tokamak fusion environment. Subsequently, the influence of neutron irradiation of EAST tokamak on the output performance of 4H-SiC p-i-n detector is studied in detail by using Silvaco TCAD. In addition, we analyzed the causes of detector performance degradation due to neutron irradiation and identified effective methods to enhance the detector's radiation tolerance.

## II. Simulation Method

### A. Neutron Yield Monitor

Although 4H-SiC detectors can detect fast neutrons through nonelastic and elastic scattering reactions with $^{12}$C and $^{28}$Si nuclei [7], their detection efficiency is not particularly high. To achieve higher detection efficiency and a flatter neutron response, a neutron fluence monitor can be constructed by putting a 4H-SiC neutron detector inside a neutron moderator made from polyethylene materials. The polyethylene materials can moderate fast neutrons into thermal neutrons. Subsequently, these thermal neutrons are detected by a 4H-SiC neutron detector coated with a $^{6}$LiF thermal neutron converter [10]. Here, 4H-SiC is used as a thermal neutron counter. The 4H-SiC detects thermal neutrons by recording the charged particles produced by thermal neutrons in the converter via the $^{6}\mathrm{Li}(n, T)\alpha$ nuclear reaction. Due to the higher energies and less energy loss in the converter, the tritons are usually used to count the incident neutrons.

For the neutron monitor, the response is defined as the triton counts recorded by 4H-SiC per unit incident neutron fluence. The response at energy $E$ is calculated by using the following formula [26]:

$$R(E) = a_s \cdot N_{6_{Li}} \sum_{i=1}^{N} c(E_i') \cdot \Phi(E_i') \cdot S(E_i') \cdot \sigma_{n,t}(E_i') \quad (1)$$

where $E$ is the incident neutron energy, $E_i'$ is represented as an array, denoting the moderated neutron energies in

the converter region, $N_{6_{Li}}$ is the $^6$Li atom number in the convertor, $a_s$ is the beam area of incident neutrons, $c(E_i')$ is the proportion of the number of tritons produced from the $^6$Li$(n, t)$ reaction and recorded by 4H-SiC detector, $\Phi(E_i')$ is the neutron fluence at the $i$th energy interval with $E_i'$ as the center, $S(E_i')$ is the neutron self-shielding factor, and $\sigma_{n,t}$ is the standard $^6$Li$(n, t)$ reaction cross section obtained from the ENDF/B-VII.0 library.

In fusion plasma experiments, it is better to characterize the damage level of 4H-SiC detector caused by neutron irradiation at different cumulative neutron yields in plasmas. First, based on the non ionizing energy loss (NIEL) hypothesis [27], we use (2) to convert the neutron fluence in the neutron monitor position into standard 1-MeV equivalent neutron fluence in the SiC crystal volume, as neutrons in the monitor position have to undergo moderation and absorption process in the moderator before irradiating the SiC crystal. Second, the transfer coefficient of the source neutrons from plasmas to the neutron monitor position should be considered. Eventually, these calculations will enable us to determine the standard 1-MeV neutron fluence level corresponding to each source neutron.

In the simulation, 4H-SiC detector is placed at the center of a cylindrical polyethylene moderator, and a 5-$\mu$m-thick $^6$LiF sample used as the thermal neutron converter was deposited on its contact surface. The surface cross-sectional dimensions of 4H-SiC detector region are 0.4 $\times$ 0.4 cm, with a thickness of 400 $\mu$m, for the purpose of detecting triton particles generated by the moderated neutrons in the converter material. In this study, we place the neutron detector at a distance of 11.0 m from the center of the tokamak and use the energy distribution of neutron fluence measured at position one in [28] as the neutron source. We then convert its fluence values to 1-MeV equivalent neutron damage fluence by using the following formula:

$$\Phi_1 = \frac{\mathrm{NIEL}(E_{\mathrm{EAST}})}{\mathrm{NIEL}(E_1)} \cdot \Phi_{\mathrm{EAST}} = k \cdot \Phi_{\mathrm{EAST}} \tag{2}$$

where $\Phi_{\mathrm{EAST}}$ is the neutron fluence generated by the EAST source at the neutron detector location, $\Phi_1$ is the 1-MeV equivalent neutron fluence at the SiC crystal volume, NIEL$(E_{\mathrm{EAST}})$ and NIEL$(E_1)$ are the nonionizing energy loss values in 4H-SiC crystal for the EAST neutron source and 1-MeV monoenergetic neutron source, respectively, and $k$ is the fluence conversion coefficient.

### B. TCAD Simulation Method

In this study, a 2-D simulation model of 4H-SiC p-i-n detector is constructed by using Silvaco TCAD to analyze the changes in the parameters, such as the sensitive region electric field, current impulse response, and CCE of the detector after neutron irradiation. The aim of the study is to investigate the degradation evolution of 4H-SiC detector performance with neutron fluence to analyze the factors of detector performance degradation and to find suitable methods that can effectively improve the irradiation resistance of the detectors.

*1) Construction of the Physical Model:* The structure of 4H-SiC detector constructed is illustrated in Fig. 1. The detector primarily consists of three parts: 1) a 350-$\mu$m-thick n+ substrate (doping = 5 $\times$ $10^{18}$ cm$^{-3}$), 2) a 50-$\mu$m-thick epitaxial layer in the $I$-region (doping = 2 $\times$ $10^{14}$ cm$^{-3}$), and 3) a 0.5-$\mu$m-thick p+ region formed on the n-type 4H-SiC epitaxial layer by Al ion implantation (doping = 1 $\times$ $10^{19}$ cm$^{-3}$), with phosphorus used as the n-type dopant. The electrodes placed at the bottom of the substrate and the top of the p+ region are designed as ohmic contacts. In TCAD simulation studies, modeling and analyzing individual detector cells is relatively easy. This approach not only ensures a sufficient grid density to enhance computational accuracy but also improves simulation efficiency [25]. Therefore, in this work, the lateral dimensions of the device structure model are set to 100 $\mu$m.

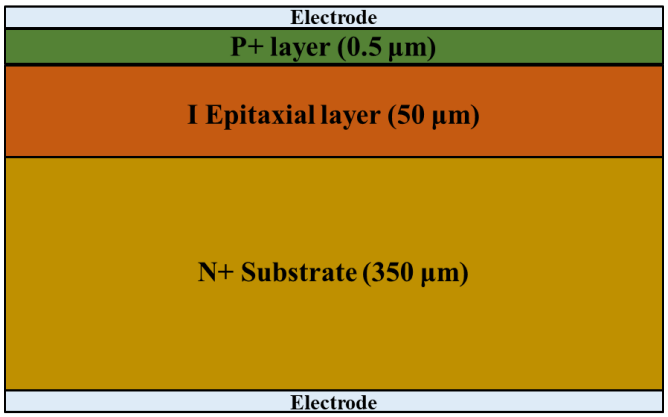


Fig. 1. Schematic of the 2-D structure of 4H-SiC p-i-n detector.

In the simulation process, in addition to considering the fundamental model, 4H-SiC material properties and basic physical models are simultaneously defined. The models used in the simulation include low-field mobility, high-field saturation, Shockley–Read–Hall (SRH) recombination, Auger recombination, impact ionization, and incomplete ionization, among others. The parameters for the models used are primarily referenced from [18].

*2) Device Damage and Particle Incidence Equivalence:* In the simulation, defect characteristic parameters in semiconductor devices, such as energy levels, concentrations, and capture cross sections, are extracted by using experimental methods, such as deep level transient spectroscopy (DLTS), thermally stimulated current (TSC), transient capacitance (TCAP), and so on [18]. These parameters are introduced into TCAD simulations using the Trap statement, and the relationship between trap density and neutron irradiation fluence is built through (3). Research indicates that fast neutron damping is the primary cause of irradiation damage during neutron detection with the detector [9], [10]. While the interaction of neutrons with the converter may generate charged particles that cause defects when they enter the detector, this effect is secondary. In this work, we primarily employ $Z1/Z2$ defects to characterize the damage caused by neutron irradiation to the detector [29]

$$N(\Phi) = N_0 + k_N \cdot \Phi \tag{3}$$

where $\Phi$ represents the radiation particle fluence, $k_N$ is the damage constantly defined as the linear relationship between

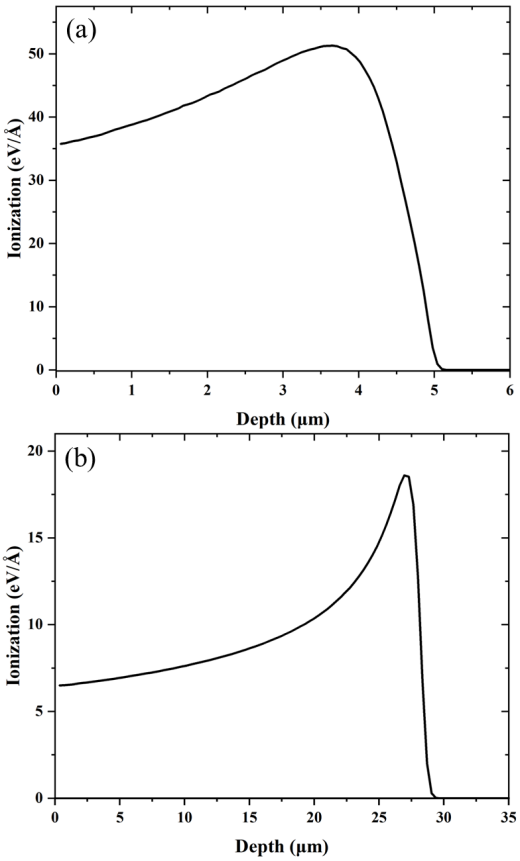


Fig. 2. Energy deposition of $\alpha$ and $T$ particles in 4H-SiC material. (a) 2.05-MeV $\alpha$ particles. (b) 2.75-MeV $T$ particles.

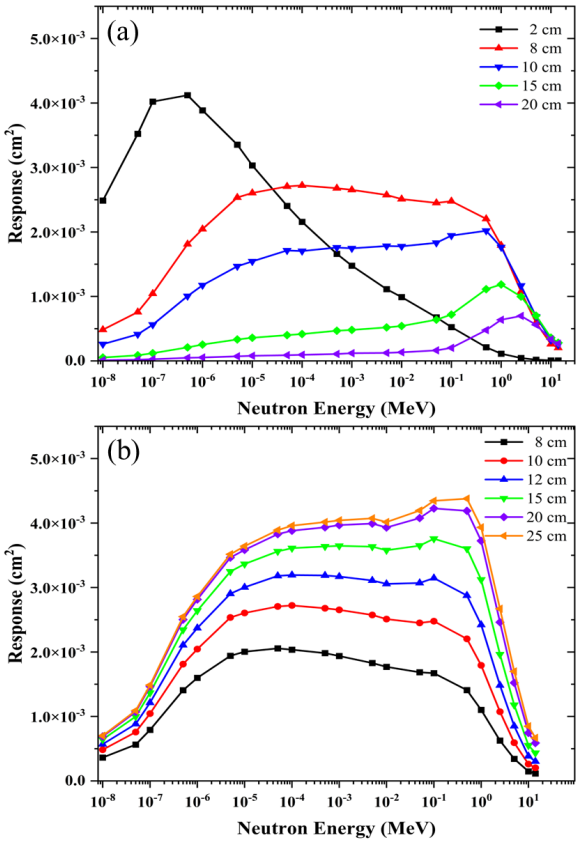


Fig. 3. Response function curves of neutron detectors with different (a) lengths and (b) diameters of polyethylene moderators.

per-unit fluence and the generation of defect quantity, and $N_0$ is the initial defect concentration before irradiation.

The secondary particles, namely, 2.73-MeV tritons and 2.05-MeV $\alpha$ particles, produced by the reactions between thermal neutrons and $^6$LiF converter will have a certain energy loss when they pass through the converter material [18], [26]. Therefore, different energies of $\alpha$ and triton particles will be incident on the p+ side of 4H-SiC detector. Only charged particles with maximum energy and vertical impingement on the detector surface are considered when calculating the energy deposition distribution within the sensitive region of the SiC crystal. Additionally, when secondary charged particles pass through the several 100-nm-thick front contact electrode, they only lose tens of kiloelectronvolts in energy. Hence, the influence of the front electrode is neglected. The energy deposition distribution of $\alpha$ and triton particles in the SiC crystal is simulated using the SRIM-2013 program, and the resulting Bragg energy distribution is depicted in Fig. 2. It is evident that the energy deposition of secondary particles in 4H-SiC crystal is highly nonuniform. Most of the particle energy is released at the end of the incident path, resulting in a sharp Bragg energy peak. Therefore, to better characterize the spatial distribution of energy deposition by secondary particles incident on the detector, a "segmentation method" is employed to describe the energy deposition [25]. For instance, for $\alpha$ particles, each segment is taken as 0.2 $\mu$m, and the average linear energy transfer (LET) value is calculated for each segment interval and used as an input for TCAD.

## III. Results and Discussion

### A. Neutron Monitor

Monte Carlo simulations were conducted to calculate the response functions of neutron monitors with different sizes of cylindrical polyethylene moderators. The results are presented in Fig. 3. We observed that the overall response values of 4H-SiC detector increase with the diameter of the polyethylene moderator. Once the diameter reaches a certain threshold, the influence of polyethylene diameter on the response diminishes. Besides, an increase in polyethylene length results in the maximum response shifting toward higher energies. For D plasma, the neutron energy spectrum around the tokamak device shows a broad energy range distribution from thermal neutrons to several megaelectronvolts. Taking the detector's detection efficiency and neutron-sensitive region into account, the optimized dimensions for the polyethylene moderator are a diameter of 20 cm and a length of 8 cm.

In the EAST fusion plasma experiment, the neutron energy spectrum measured at a distance of 11.0 m from the tokamak center [28] is shown in Fig. 4(a). Using it as the neutron source, the neutron energy spectrum incident on the surface of the 4H-SiC detector after passing through the designed detector moderator is depicted in Fig. 4(b). Based on the NIEL assumption, using (2), the equivalent conversion coefficient $k$

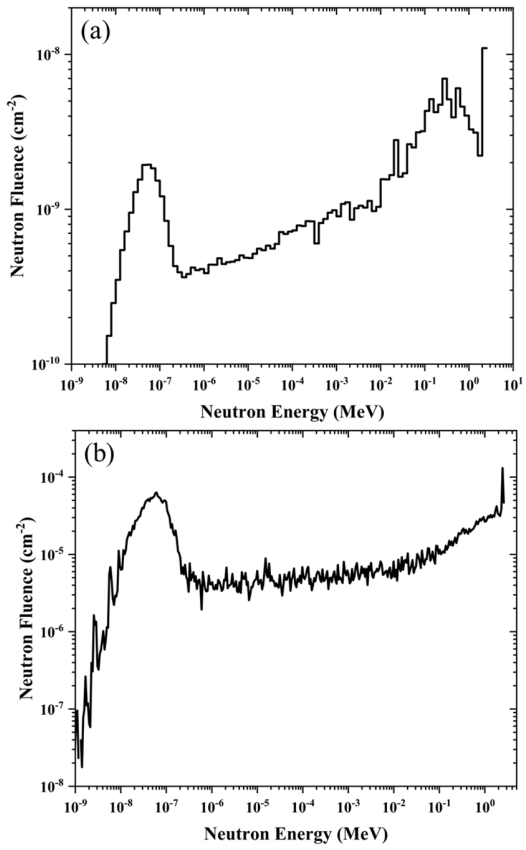


Fig. 4. Neutron spectrum in the EAST D plasma experiment. Neutron energy spectrum at (a) distance of 11 m from the tokamak and (b) position of the SiC volume of the neutron monitor.

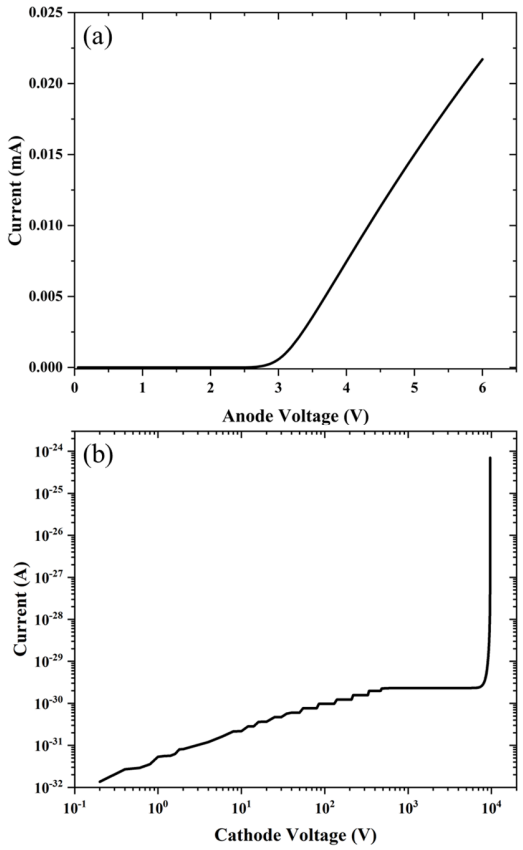


Fig. 5. *I–V* characteristics of 4H-SiC detector before neutron irradiation. (a) Forward *I–V* curve. (b) Reverse breakdown voltages.

for the neutron fluence $\Phi_{\mathrm{EAST}}$ at this location is determined to be 0.916. Considering the transmission coefficient from the source neutrons to the neutron monitor location to be approximately $1.4 \times 10^{-7}$ cm$^{-2}$ per source neutrons [28], the 1-MeV equivalent neutron damage fluence at the SiC crystal volume for one source neutrons emitted from plasmas is determined to be $1.28 \times 10^{-7}$ cm$^{-2}$.

### B. Characteristics of the Unirradiated 4H-SiC p-i-n Detector

Silvaco TCAD was utilized to simulate the forward $I$–$V$ curves and reverse breakdown voltages of 4H-SiC p-i-n detector, as depicted in Fig. 5. We observed that the forward threshold voltage of the detector is approximately 2.7 V, while the reverse breakdown voltage is around 9000 V.

Further analysis of the relationship between the thickness of the detector's sensitive region and the applied operating bias voltage is presented in the simulation results in Fig. 6. We observed that there is a positive correlation between the thickness of the detector's sensitive region and the operating bias voltage. The maximum thickness of the sensitive region is similar to the thickness of the detector's intrinsic region ($I$ region). After the thickness of the detector's sensitive region reaches its maximum, an increase of operating bias voltage can merely strengthen the electric field in the sensitive region, without changing the thickness of the sensitive region. The simulation results are consistent with the calculations in [25].

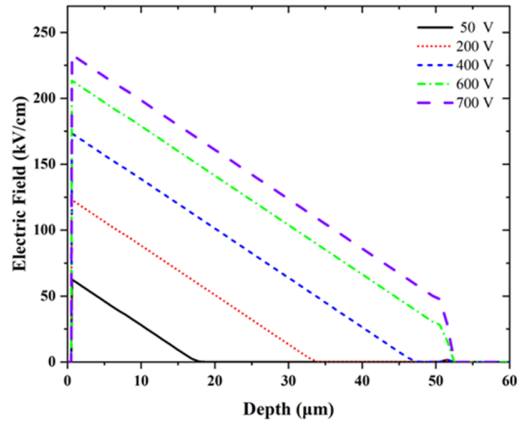


Fig. 6. Electric field distribution in the sensitive region of 4H-SiC detector at different operating bias voltages.

Since the drift motion of charge carriers generated by secondary particles within the sensitive region is the primary source of the detector's output signal, it is essential that the depleted region width is greater than the maximum penetration range of incoming particles inside the SiC sensitive region. As shown in Fig. 2(b), the maximum range of 2.73-MeV triton particles within 4H-SiC detector is approximately 28 $\mu$m. As evident from Fig. 6, when the operating bias voltage is 200 V, the active layer thickness of 4H-SiC detector is about 33 $\mu$m. Therefore, for the subsequent simulation process, the

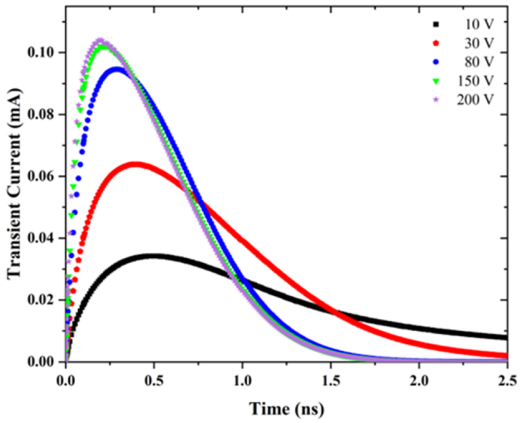


Fig. 7. Transient current pulse response of 4H-SiC detector to 2.05-MeV $\alpha$ particles at different operating bias voltages.

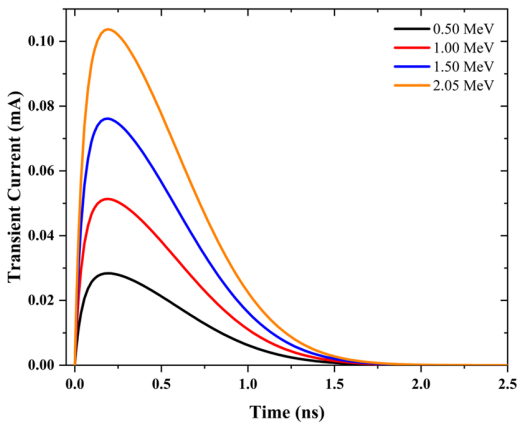


Fig. 8. Transient current pulse response of 4H-SiC detector to $\alpha$ particles of different energies at 200-V operating bias voltage.

operating bias voltage was set to 200 V to ensure an adequate depletion region thickness.

The influence of operating bias voltage on the detector's output characteristics was further analyzed. The simulations were performed for 2.05-MeV $\alpha$ particles under different operating bias voltages, and the resulting changes in the detector's output current pulse waveform are depicted in Fig. 7. We observed that the output signal has a width in the nanosecond range, indicating a fast response in 4H-SiC detector. This allows it to operate in pulse mode for monitoring intense neutron fields.

As the operating bias voltage increases, the width of the detector's output current pulse waveform decreases, and the peak position increases. At lower operating bias voltages, there is a noticeable tailing effect in the detector's output current pulse. However, when the operating bias voltage exceeds 150 V, an increase in the operating bias voltage results in the detector's output waveform remaining essentially unchanged. This is because at lower operating bias voltages, the depletion layer thickness and field strength in the detector are relatively small. Besides, as can be seen from Fig. 2, the range of $\alpha$ particles with an energy of 2.05 MeV is about 5 $\mu$m in the detector. They deposit a significantly greater amount of energy in the latter half of their trajectory, which is the primary region for generating charge carriers. Therefore, when the depletion layer is relatively thin, some of the charge carriers are generated outside the depletion region. Because there is virtually no electric field outside the depletion region, these charge carriers do not contribute to the detector's output signal. Additionally, under lower field strengths, the drift velocity of charge carriers is slower, resulting in a wider pulsewidth. By increasing the operating voltage, when the depletion layer thickness is greater than the range of incoming particles, almost all charge carriers are generated within the depletion layer. At the same time, there is a high-field saturation phenomenon in the carrier drift velocity. Therefore, when the operating bias voltage reaches a certain level, the detector's current pulse response remains essentially unchanged.

When choosing a depletion layer thickness that is sufficient, i.e., with an operating bias of 200 V, the changes in the output current pulse waveform of 4H-SiC p-i-n detector when

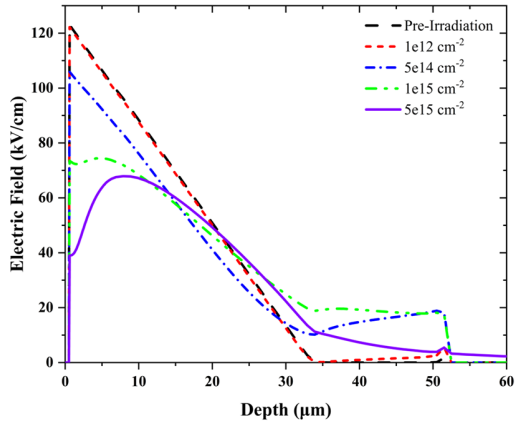


Fig. 9. Electric field distribution in the sensitive region of 4H-SiC detector at 200-V operating bias voltage for different neutron fluence levels.

detecting $\alpha$ particles of different energies were investigated, as shown in Fig. 8. The simulation results indicate that as the $\alpha$-particle energy increases, the peak of the transient current pulse rises, and the pulsewidth can see a slight increase. This is because the charge carriers generated by secondary particles are primarily within the sensitive region. As the energy of incident $\alpha$ particles increases, the number of charge carriers generated inside the detector also has the same trend. Furthermore, since charge carriers are predominantly generated at the end of the particle's trajectory, and the higher incident particle energies, the longer the corresponding particle ranges are, the pulsewidth slightly increases with the increase of incident particle energy.

### C. Characteristics of the Neutron-Irradiated 4H-SiC p-i-n Detector

Shown in Fig. 9 are the electric field distributions in the sensitive region of the SiC crystal at 200-V operating bias voltage after being irradiated with different neutron fluences of 1 MeV. When the neutron fluence increases, there is a distortion in the electric field distribution within the detector's sensitive region, particularly at both ends of the sensitive region. This is due to a large number of defects within the

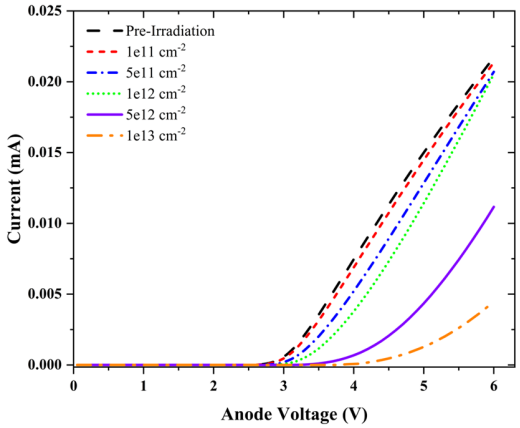


Fig. 10. *I–V* characteristics curves of 4H-SiC detector under different neutron irradiation fluences.

detector due to neutron radiation damage. When the charge carriers generated by the incident $\alpha$ particles drift within the sensitive region under the influence of the electric field, these defects have a certain probability of capturing the charge carriers, turning them from neutral into charged. This, in turn, creates an internal electric field and alters the electric field distribution within the detector's sensitive region.

Fig. 10 shows the forward $I$–$V$ characteristics of 4H-SiC detector irradiated with different amounts of incident neutrons. The curve tends to shift to the right with increasing neutron irradiation fluence compared with the unirradiated detector.

This is due to the fact that neutron irradiation produces defects that change the material properties and junction characteristics of 4H-SiC detector. The simulated device is no longer an ideal semiconductor device, and this leads to the generation of a new leakage mechanism, thereby altering the conduction mechanism of the device. This change may lead to increased noise in experimental measurements.

At an operating bias voltage of 200 V, the detector's response to 0.5-MeV $\alpha$ particles was further analyzed after exposure to different fluences of 1-MeV neutrons. The simulation results are presented in Fig. 11(a). With the increase in neutron fluence, the peak current of the detector's output current pulses decreases, and the peak position also changes. It is worth noting that at a neutron fluence of $1 \times 10^{12}$ cm$^{-2}$, while the current pulse signal experiences some attenuation (with a CCE of 96%, as shown in Fig. 12) and waveform distortion, the changes in the detector's sensitive region electric field (as shown in Fig. 9) are not very significant. There are only slight variations in the field strength at both ends, indicating that the pulse shape is highly sensitive to changes in the sensitive region's electric field. Furthermore, as shown in Fig. 11(b), when the neutron fluence is relatively high, the output signal pulsewidth becomes narrower. This is due to the neutron irradiation, as shown in Fig. 9, causing changes in the sensitive region's electric field, affecting the drift velocity of charge carriers, and thereby impacting the detector's output current pulse signal. From Fig. 11(a), we observed that when the neutron fluence is greater than $1 \times 10^{11}$ cm$^{-2}$, the current pulse shape changes significantly with increasing neutron fluence. Therefore, in experimental

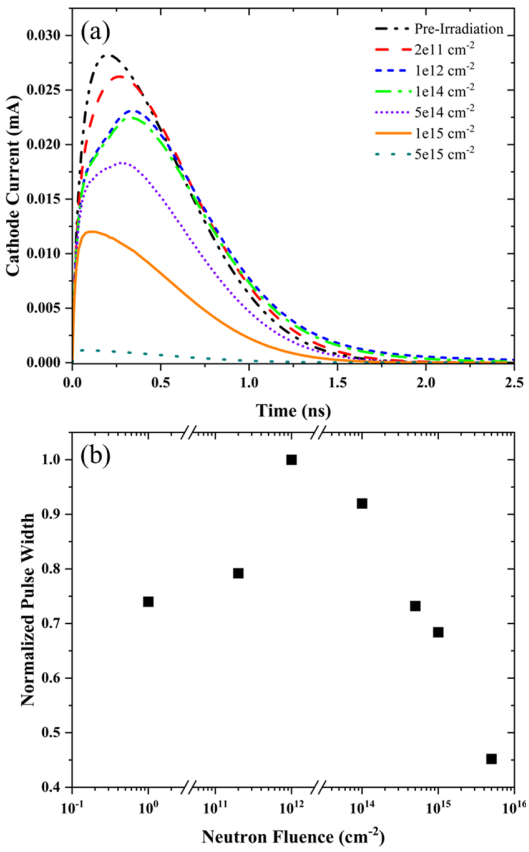


Fig. 11. (a) Transient current pulse response and (b) pulsewidth of the 4H-SiC detector to 0.5-MeV $\alpha$ particles at 200-V operating bias after neutron irradiation under different neutron fluences.

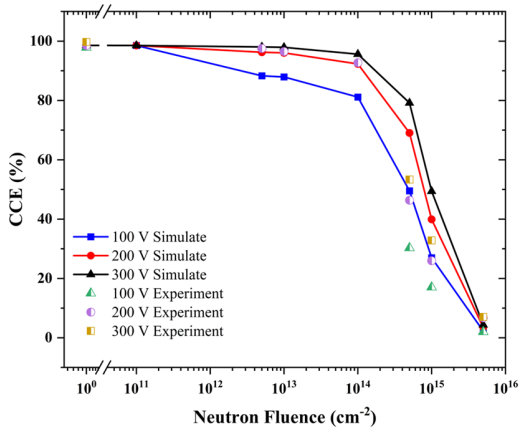


Fig. 12. CCEs of 4H-SiC detector at different operating biases and after neutron irradiation under different fluences.

measurements, analyzing the shape of the current pulses from 4H-SiC detector may be used to estimate the levels of incident neutron fluence and changes in SiC detector property parameters like CCE.

Next, the impact of operating bias voltage on the radiation stability of the detector was analyzed. Simulations were conducted at operating bias voltages of 100, 200, and 300 V. The detector was used to detect 0.5-MeV $\alpha$ particles following irradiation with varying neutron fluences, and the changes in the output current pulse waveforms were observed. We observed that under nonirradiated conditions, the output

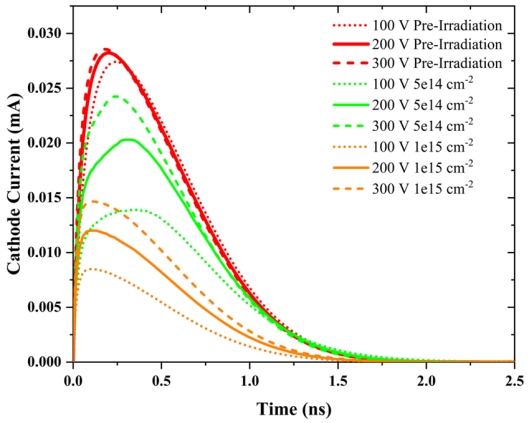


Fig. 13. Transient current pulse response of 4H-SiC detector to 0.5-MeV $\alpha$ particles at different operating bias voltages after the neutron irradiation under different fluences.

signals are nearly identical at different operating bias voltages. After exposure to a certain neutron fluence, the detector's output current pulse signals exhibit peak and shape changes similar to those seen in Fig. 13. At the same time, we observed that as the operating bias voltage increases, the variations in the detector's output waveform show a downward trend, indicating an enhanced radiation stability in the detector. This is because higher operating bias voltage intensifies the electric field in the detector's sensitive region, leading to the increased carrier mobility and making it more challenging for carriers to be captured. Consequently, the internal electric field generated by defect-captured carriers weakens, reducing the probability of carrier recombination. Therefore, during detector operation, maximizing the operating bias voltage is an effective approach to enhance the detector's radiation tolerance.

Finally, the impact of neutron irradiation on the CCE of 4H-SiC detector is depicted in Fig. 12. We observed that simulation results and experimental measurements exhibit good agreement at neutron fluences below $1 \times 10^{14}$ cm$^{-2}$. In the high neutron fluence region, the simulation results slightly exceed the experimental values [16]. This is primarily due to the idealized parameter settings used in the simulation, resulting in slightly higher simulated CCE values than the experimental data. From Fig. 12, it is evident that as the neutron irradiation fluence increases, the CCE of the detector decreases. For instance, at an operating bias voltage of 200 V, when the neutron irradiation fluence reaches $1 \times 10^{14}$ cm$^{-2}$, the CCE still has 94%. We also experimentally investigate the neutron damage of the SiC detector using an accelerator neutron source. It is observed that the output performance of the 4H-SiC detector remains almost unchanged at a neutron irradiation fluence of $1 \times 10^{14}$ cm$^{-2}$ [30]. However, with an irradiation fluence of $1 \times 10^{15}$ cm$^{-2}$, the CCE drops significantly to only 40%. Similarly, as seen in Fig. 12, increasing the operating voltage of the detector can effectively mitigate the decrease in the CCE. This further illustrates that raising the operating voltage of the detector can significantly offset the effects of its exposure to neutron irradiation. At an operating voltage of 300 V, even when the neutron irradiation level reaches $5 \times 10^{14}$ cm$^{-2}$, the detector's CCE remains at 79%. Therefore, at an operating voltage of 300 V, even when the neutron yield from the source reaches $3.91 \times 10^{21}$ neutrons, the designed detector can still be stably used at a distance of 11 m from the tokamak. Furthermore, during a typical plasma discharge generated by neutral beam heating (Shot #101896) at EAST, approximately $1.7 \times 10^{15}$ neutrons were produced [7].

As a result, it can be concluded that 4H-SiC detectors in this study are capable of withstanding more than $2.3 \times 10^{6}$ plasma discharge experiments when operating at an operating bias voltage of 300 V.

However, for fusion experiments with higher neutron yields, such as the International Thermonuclear Experimental Reactor (ITER) deuterium-tritium (DT) plasma experiment where the neutron yield exceeds $10^{19}$ s$^{-1}$ and is ~five orders of magnitude higher than that in the EAST D plasma experiment [6], [7], the neutron radiations might lead to a significant degradation of 4H-SiC detector performance after several neutron discharges. Therefore, for higher neutron fluences (exceeding $10^{15}$ cm$^{-2}$ for example), a comprehensive analysis of the distortion of the pulse-height spectrum of the 4H-SiC detector due to neutron damage is needed to determine whether or not the detectors are stable enough for plasma diagnostics [9], [10], [11], [31]. This will be investigated in subsequent work.

## IV. Conclusion and Outlook

This work optimized a 4H-SiC p-i-n detector-based neutron monitor for fusion neutron detection using the MCNP code. Additionally, we utilized Silvaco TCAD simulations to investigate the output performance of 4H-SiC p-i-n detectors due to high fluence of neutron damage. The predicted CCE values are in a good agreement with the experimental results for neutron fluences up to $5 \times 10^{15}$ cm$^{-2}$. The results of the research indicate that 4H-SiC detectors possess excellent performance and a strong tolerance to neutron irradiation. At low neutron fluences, such as $1 \times 10^{12}$ cm$^{-2}$, the detector's output current pulses show minor fluctuations, but there is relatively little change in the electric field within the sensitive region and the CCE. However, when being exposed to a higher neutron fluence, 4H-SiC detector exhibits performance degradation similar to that of a diamond detector, with a noticeable change in the detector's output signal. At an operating bias voltage of 200 V and without irradiation, the detector has a CCE value of 98.5%. After equivalent 1-MeV neutron irradiation at a fluence of $1 \times 10^{14}$ cm$^{-2}$, the CCE value only decreases by 5%, demonstrating excellent radiation tolerance. However, at a neutron irradiation of $1 \times 10^{15}$ cm$^{-2}$, the detector exhibits a substantial degradation in device performance, with the CCE value dropping to only 40%. Furthermore, the research indicates that the irradiation-induced degradation of detector performance is primarily attributed to irradiation defects, which capture space charge, resulting in a reduced electric field within the sensitive region and an increase in charge carrier recombination. At the same time, through simulation studies, it has been observed that increasing the operating bias voltage to elevate the drift velocity of charge carriers within the detector can effectively enhance the detector's resistance to neutron irradiation.

The SiC detectors have a higher resistance to neutron damage than the diamond detectors, which can be used to develop neutron monitors and neutron spectrometers for fusion plasma diagnosing [10], [12], [31], [32], [33]. In addition, when measuring 14-MeV DT fusion neutrons using the SiC detectors, similar to the diamond detector, in the pulse height spectra, an isolated peak due to $^{12}C(n, \alpha)^{9}Be$ reactions is far away from the background and other complex structures. The single isolated peak might be well suited for DT plasma diagnostic studies like the diamond detectors [31], [34]. Besides, SiC detectors are far cheaper than diamond detectors [1], [9]. Therefore, in future research, based on the results of the present study, we further try to reconstruct the experimental pulse height spectra of the SiC detectors used in fusion neutrons detection. Then, we will analyze the influence of the shape distortion of the pulse height spectra on the neutron yield monitor and fast ions-related plasma diagnostics in tokamaks.

## REFERENCES


[1] J. M. Gómez-Ros, "Solid state detectors for neutron radiation monitoring in fusion facilities," *Radiat. Meas.*, vol. 71, pp. 421–424, Dec. 2014, doi: 10.1016/j.radmeas.2014.05.003.

[2] A. Murari et al., "'Burning plasma' diagnostics for the physics of JET and ITER," *Plasma Phys. Controlled Fusion*, vol. 47, no. 12B, pp. B249–B262, Dec. 2005, doi: 10.1088/0741-3335/47/12B/S19.

[3] A. Murari et al., "New developments in the diagnostics for the fusion products on JET in preparation for ITER (invited)," *Rev. Sci. Instrum.*, vol. 81, no. 10, Oct. 2010, Art. no. 10E136, doi: 10.1063/1.3502038.

[4] M. Angelone et al., "Development of single crystal diamond neutron detectors and test at JET tokamak," *Nucl. Instrum. Methods Phys. Res. A, Accel. Spectrom. Detect. Assoc. Equip.*, vol. 595, no. 3, pp. 616–622, Oct. 2008, doi: 10.1016/j.nima.2008.07.107.

[5] M. Sasao, L. Bertalot, M. Ishikawa, and S. Popovichev, "Strategy for the absolute neutron emission measurement on ITER," *Rev. Sci. Instrum.*, vol. 81, no. 10, p. 1503, Oct. 2010, doi: 10.1063/1.3491049.

[6] L. Bertalot et al., "Present status of ITER neutron diagnostics (don't short) development," *J. Fusion Energy*, vol. 38, nos. 3–4, pp. 283–290, Jul. 2019, doi: 10.1007/s10894-019-00220-w.

[7] B. Hong et al., "Diagnostic of fusion neutrons on EAST tokamak using 4H-SiC detector," *IEEE Trans. Nucl. Sci.*, vol. 69, no. 3, pp. 639–644, Mar. 2022, doi: 10.1109/TNS.2022.3146180.

[8] V. Krasilnikov, L. Bertalot, R. Barnsley, and M. Walsh, "Neutron detector needs for ITER," *Fusion Sci. Technol.*, vol. 71, no. 2, pp. 196–200, Feb. 2017, doi: 10.13182/FST16-108.

[9] F. H. Ruddy, L. Ottaviani, A. Lyoussi, C. Destouches, O. Palais, and C. Reynard-Carette, "Silicon carbide neutron detectors for harsh nuclear environments: A review of the state of the art," *IEEE Trans. Nucl. Sci.*, vol. 69, no. 4, pp. 792–803, Apr. 2022, doi: 10.1109/TNS.2022.3144125.

[10] M. De Napoli, "SiC detectors: A review on the use of silicon carbide as radiation detection material," *Frontiers Phys.*, vol. 10, Oct. 2022, Art. no. 898833, doi: 10.3389/fphy.2022.898833.

[11] P. V. Raja, "Performance studies of silicon and 4H-silicon carbide radiation detectors for fusion plasma diagnostics," Ph.D. dissertation, Dept. Elect. Sci., IIT, Bhubaneswar, India, 2019.

[12] L. Liu, F. Li, S. Bai, P. Jin, X. Cao, and X. Ouyang, "Silicon carbide PIN diode detectors used in harsh neutron irradiation," *Sens. Actuators A, Phys.*, vol. 280, pp. 245–251, Sep. 2018, doi: 10.1016/j.sna.2018.07.053.

[13] M. Hodgson, A. Lohstroh, P. Sellin, and D. Thomas, "Characterization of silicon carbide and diamond detectors for neutron applications," *Meas. Sci. Technol.*, vol. 28, no. 10, Sep. 2017, Art. no. 105501, doi: 10.1088/1361-6501/aa7f8b.

[14] R. L. Gao et al., "Radiation tolerance analysis of 4H-SiC PIN diode detectors for neutron irradiation," *Sens. Actuators A, Phys.*, vol. 333, Jan. 2022, Art. no. 113241, doi: 10.1016/j.sna.2021.113241.

[15] F. Moscatelli et al., "Radiation hardness after very high neutron irradiation of minimum ionizing particle detectors based on 4H-SiC $p^{+}n$ junctions," *IEEE Trans. Nucl. Sci.*, vol. 53, no. 3, pp. 1557–1563, Feb. 2006, doi: 10.1109/TNS.2006.872202.

[16] P. Gaggl et al., "Performance of neutron-irradiated 4H-silicon carbide diodes subjected to alpha radiation," *J. Instrum.*, vol. 18, no. 1, Jan. 2023, Art. no. C01042, doi: 10.1088/1748-0221/18/01/C01042.

[17] J. Vobecký, P. Hazdra, V. Záhlava, A. Mihaila, and M. Berthou, "ON-state characteristics of proton irradiated 4H–SiC Schottky diode: The calibration of model parameters for device simulation," *Solid-State Electron.*, vol. 94, pp. 32–38, Apr. 2014, doi: 10.1016/j.sse.2014.02.004.

[18] S. Tripathi, C. Upadhyay, C. P. Nagaraj, A. Venkatesan, and K. Devan, "The performance simulation of the LiH-SiC-based fast neutron detector for harsh environment monitoring using Geant4 and TCAD," *Nucl. Instrum. Methods Phys. Res. A, Accel. Spectrom. Detect. Assoc. Equip.*, vol. 916, pp. 246–256, Feb. 2019, doi: 10.1016/j.nima.2018.10.202.

[19] *ATLAS User's Manual: Device Simulation Software, Version 5.15.32. R*, Silvaco, Santa Clara, CA, USA, 2015.

[20] C. Jain et al., "Modeling of neutron radiation-induced defects in silicon particle detectors," *Semicond. Sci. Technol.*, vol. 35, no. 4, Mar. 2020, Art. no. 045021, doi: 10.1088/1361-6641/ab74ea.

[21] F. Kassel, M. Guthoff, A. Dabrowski, and W. de Boer, "Severe signal loss in diamond beam loss monitors in high particle rate environments by charge trapping in radiation-induced defects," *Phys. Status Solidi A*, vol. 213, no. 10, pp. 2641–2649, Jul. 2016, doi: 10.1002/pssa.201600185.

[22] H. Huang, X. Tang, H. Guo, Y. Zhang, Y. Zhang, and Y. Zhang, "Design and spectrum calculation of 4H-SiC thermal neutron detectors using FLUKA and TCAD," *Nucl. Instrum. Methods Phys. Res. A, Accel. Spectrom. Detect. Assoc. Equip.*, vol. 833, pp. 192–198, Oct. 2016, doi: 10.1016/j.nima.2016.06.120.

[23] A. Siddiqui and M. Usman, "Radiation tolerance comparison of silicon and 4H–SiC Schottky diodes," *Mater. Sci. Semicond. Process.*, vol. 135, Nov. 2021, Art. no. 106085, doi: 10.1016/j.mssp.2021.106085.

[24] Y. Xiong et al., "Simulation of the charge collection characteristics of the 4H-SiC PIN fast neutron detector with TCAD," in *Proc. 9th Symp. Novel Photoelectronic Detection Technol. Appl.*, Apr. 2023, doi: 10.1117/12.2662918.

[25] L. Zhang et al., "Transient current analysis of silicon carbide neutron detector using SRIM and TCAD," *IEEE Sensors J.*, vol. 22, no. 11, pp. 10620–10629, Jun. 2022, doi: 10.1109/JSEN.2022.3170570.

[26] Z. M. Hu et al., "An active bonner sphere spectrometer capable of intense neutron field measurement," *Appl. Phys. Lett.*, vol. 114, no. 23, Jun. 2019, Art. no. 233502, doi: 10.1063/1.5096191.

[27] M. Moll, "Radiation damage in silicon particle detectors: Microscopic defects and macroscopic properties," Ph.D. dissertation, DESY, TIB, Hannove, Germany, 1999.

[28] Z. Hu et al., "Neutron field measurement at the experimental advanced superconducting tokamak using a bonner sphere spectrometer," *Nucl. Instrum. Methods Phys. Res. A, Accel. Spectrom. Detect. Assoc. Equip.*, vol. 895, pp. 100–106, Jul. 2018, doi: 10.1016/j.nima.2018.04.010.

[29] P. Hazdra, S. Popelka, and V. Zahlava, "The influence of neutron irradiation on electrical characteristics of 4H-SiC power devices," *Mater. Sci. Forum*, vols. 821–823, pp. 785–788, Jun. 2015, doi: 10.4028/www.scientific.net/MSF.821-823.785.

[30] J. Song et al., "Development of a silicon carbide radiation detection system and experimentation of the system performance," *Appl. Radiat. Isot.*, submitted for publication.

[31] M. Rebai et al., "New thick silicon carbide detectors: Response to 14 MeV neutrons and comparison with single-crystal diamonds," *Nucl. Instrum. Methods Phys. Res. A, Accel. Spectrom. Detect. Assoc. Equip.*, vol. 946, Dec. 2019, Art. no. 162637, doi: 10.1016/j.nima.2019.162637.

[32] M. Angelone and C. Verons, "Properties of diamond-based neutron detectors operated in harsh environments," *J. Nucl. Eng.*, vol. 2, no. 4, pp. 422–470, Oct. 2021, doi: 10.3390/.jne2040032.

[33] M. Passeri et al., "Assessment of single crystal diamond detector radiation hardness to 14 MeV neutrons," *Nucl. Instrum. Methods Phys. Res. A, Accel. Spectrom. Detect. Assoc. Equip.*, vol. 1010, Sep. 2021, Art. no. 165574, doi: 10.1016/j.nima.2021.165574.

[34] O. Obraztsova, L. Ottaviani, A. Klix, T. Döring, O. Palais, and A. Lyoussi, "Comparing the response of a SiC and a sCVD diamond detectors to 14-MeV neutron radiation," *IEEE Trans. Nucl. Sci.*, vol. 65, no. 9, pp. 2380–2384, Sep. 2018, doi: 10.1109/TNS.2018.2848469.


**Yongbo Sun** is currently pursuing the M.Eng. degree in nuclear science and technology with the Department of Nuclear Science and Technology, Nanjing University of Aeronautics and Astronautics, Nanjing, China.

His research focuses on exploring the performance degradation evolution of SiC detectors in intense radiation fields, analyzing the causes of performance degradation, and studying radiation hardening methods.

**Zhimeng Hu** received the B.S. degree from Lanzhou University, Lanzhou, China, in 2012, and the Ph.D. degree from Peking University, Beijing, China, in 2017, both in nuclear physics and particle physics.

From 2017 to 2018, he was a Postdoctoral Researcher with Peking University, and the University of Milan-Bicocca, Milan, Italy, from 2018 to 2021. He is currently an Associate Professor with the Department of Nuclear Science and Technology, Nanjing University of Aeronautics and Astronautics, Nanjing, China. His research interests include radiation detection methods and instruments and the neutron measurements for fusion plasmas diagnostics.

**Hui Zhang** received the B.Eng. degree in automatic control engineering from the Huazhong University of Science and Technology, Wuhan, China, in 1992.

He is currently an Associate Researcher with the National Institute of Metrology, Beijing, China. His research interests include neutron measurement and metrology, dosimetry, and nuclear electronics.

**Pin Gong** received the B.Eng. degree in nuclear physics and nuclear technology from Nanjing University, Nanjing, China, in 2002, and the D.Eng. degree in nuclear technology and material engineering from the Nanjing University of Aeronautics and Astronautics, Nanjing, in 2022.

He is currently an Associate Professor with the Department of Nuclear Science and Technology, Nanjing University of Aeronautics and Astronautics. His research interests include advanced particle detection and electronics.

**Guoqiang Zhong** received the B.Eng. degree in nuclear engineering and technology from the University of South China, Hengyang, China, in 2005, and the Ph.D. degree from the University of Science and Technology of China (USTC), Hefei, China, in 2018.

From 2005 to 2012, he was engaged in tokamak magnetic confinement fusion experimental research with the Institute of Plasma Physics, Chinese Academy of Sciences (ASIPP), Hefei, and is responsible for neutron and gamma ray diagnostics. Since 2012, he has been mainly engaged in research related to fusion nuclear radiation monitoring and protection in ASIPP. He is currently an Associate Researcher with ASIPP.

**Liqun Hu** received the B.Eng. degree in electron beam ion beam equipment and technology from Xi'an Jiaotong University, Xi'an, China, in 1984, and the Ph.D. degree in plasma physics from the Institute of Plasma Physics, Chinese Academy of Sciences, Hefei, China, in 1992.

From 1996 to 1998, he was a Visiting Scholar with the Institute of Plasma Physics, Max Planck Association, Munich, Germany. From 1998 to 1999, he was a Visiting Scholar with the Japan Institute of Atomic Force, Kyoto, Japan. He is currently a Researcher with the Institute of Plasma Physics, Chinese Academy of Sciences.

**Giuseppe Gorini** received the B.S. (cum laude) degree from Pisa University, Pisa, Italy, and Scuola Normale Superiore, Pisa, in 1985, and the Ph.D. (cum laude) degree from Scuola Normale Superiore, in 1991, both in physics.

For the past 30 years, he was engaged in the development of new experimental methods for neutron measurements in fusion and material science. He is presently a Full Professor with the Department of Physics, University of Milan-Bicocca, Milan, Italy. His scientific production is documented more than 800 journal articles.

**Gabriele Croci** received the B.S. (cum laude) degree from the University of Milan-Bicocca, Milan, Italy, in 2007, and the Ph.D. (cum laude) degree from the University of Siena, Siena, Italy, in 2011, both in physics.

He is presently an Associate Professor with the Department of Physics, University of Milan-Bicocca. For the past 15 years, he was engaged in the development of new experimental devices for neutron, gamma ray, and X-rays measurements in fusion and spallation sources-related experiments. His scientific production is documented in more than 500 journal articles.

**Xiaobin Tang** received the B.Eng. degree in materials science and engineering and the D.Eng. degree in test metrology technologies and instruments from the Nanjing University of Aeronautics and Astronautics, Nanjing, China, in 2000 and 2009, respectively.

He is currently a Full Professor with the Department of Nuclear Science and Technology, Nanjing University of Aeronautics and Astronautics. He published more than 200 research articles. His research interests include nuclear technology and applications mainly in medical physics, energy, space communication, and nuclear emergency.